CHEMISTRY
A EUROPEAN JOURNAL

DOI: 10.1002/chem.200600040

Chemical Radiation Studies of 8-Bromo-2′-deoxyinosine and 8-Bromoinosine in Aqueous Solutions

Marialuisa Russo,[a] Liliana B. Jimenez,[a, b] Quinto G. Mulazzani,[a] Mila D'Angelantonio,[a] Maurizio Guerra,[a] Miguel A. Miranda,[b] and Chryssostomos Chatgilialoglu*[a]

Abstract: The reactions of hydrated electrons (e_{aq}^-) with 8-bromo-2′-deoxyinosine (**8**) and 8-bromoinosine (**12**) have been investigated by radiolytic methods coupled with product studies and have been addressed computationally by means of BB1K-HMDFT calculations. Pulse radiolysis revealed that one-electron reductive cleavage of the C–Br bond gives the C8 radical **9** or **13** followed by a fast radical translocation to the sugar moiety. Selective generation of a C5′ radical occurs in the 2′-deoxyribo derivative, whereas in the ribo analogue the reaction is partitioned between the C5′ and C2′ positions with similar rates. Both C5′ radicals undergo cyclizations, **10**→**11** and **14**→**15**, with rate constants of 1.4×10^5 and of $1.3\times10^4\ s^{-1}$, respectively. The redox properties of radicals **10** and **11** have also been investigated. A synthetically useful photoreaction has also been developed as a one-pot procedure that allows the conversion of **8** to 5′,8-cyclo-2′-deoxyinosine in a high yield and a diastereoisomeric ratio (5′*R*)/(5′*S*) of 4:1. The present results are compared with data previously obtained for 8-bromoadenine and 8-bromoguanine nucleosides. Theory suggests that the behavior of 8-bromopurine derivatives with respect to solvated electrons can be attributed to differences in the energy gap between the π*- and σ*-radical anions.

Keywords: cyclization · density functional calculations · nucleosides · pulse radiolysis · radical reactions

Introduction

The reactions of hydrated electrons (e_{aq}^-) with 8-bromoadenine[1–3] and 8-bromoguanine nucleosides[4–6] have recently been investigated by radiolytic methods. It was found that 8-bromo-2′-deoxyadenosine (**1**) captures electrons and rapidly loses a bromide ion to give the corresponding C8 radical **2**. This intermediate intramolecularly abstracts a hydrogen atom from the C5′ position to selectively afford the 2′-deoxyadenosin-5′-yl radical **3** (Scheme 1).[1,2,7] This allowed the reactivity of **3** to be studied properly for the first time, particularly the cyclization step **3**→**4**, which occurs with a rate constant (k_c) of $1.6\times10^5\ s^{-1}$. In the analogous reaction with 8-bromoadenosine, the intramolecular hydrogen abstraction by the initially formed C8 radical is partitioned between two channels to generate both the C5′ and C2′ radicals with similar rate constants.[3] On the other hand, 8-bromo-2′-deoxyguanosine (**5**) captures electrons with the formation of radical anion **6** that undergoes protonation at C8 to afford the one-electron oxidized 2′-deoxyguanosine **7**.[6] Similar reactions have been observed with 8-bromoguanosine.[4,5]

Information on the two distinct reaction paths was also obtained by means of UB3LYP/6-31G* calculations. In the frozen radical anion of **1** the unpaired electron is substantially localized at C8 and, upon relaxation of the structural parameters, the unpaired electron tends to occupy the antibonding $\sigma^*_{C8\text{-}Br}$ molecular orbital favoring the loss of Br^- and formation of radical **2**.[2] On the other hand, radical anion **6** is computed to be stable and is found to be protonated at C8 with loss of Br^- to give radical **7**.[5,6]

8-Bromo derivatives **1** and **5** were also incorporated in a variety of single- or double-stranded oligonucleotides and G quadruplexes as a detection system for excess electron-transfer processes.[8–11] Interestingly, the 8-bromo-2′-deoxyadenosine moieties in a series of DNA hairpins containing a

[a] Dr. M. Russo, L. B. Jimenez, Dr. Q. G. Mulazzani, Dr. M. D'Angelantonio, Dr. M. Guerra, Dr. C. Chatgilialoglu
ISOF, Consiglio Nazionale delle Ricerche
Via P. Gobetti 101, 40129 Bologna (Italy)
Fax: (+39) 051-639-8349
E-mail: chrys@isof.cnr.it

[b] L. B. Jimenez, Prof. M. A. Miranda
Departamento de Quimica, Universidad Politécnica de Valencia
Camino de Vera s/n, 46022 Valencia (Spain)

Supporting information for this article is available on the WWW under http://www.chemeurj.org/ or from the author.

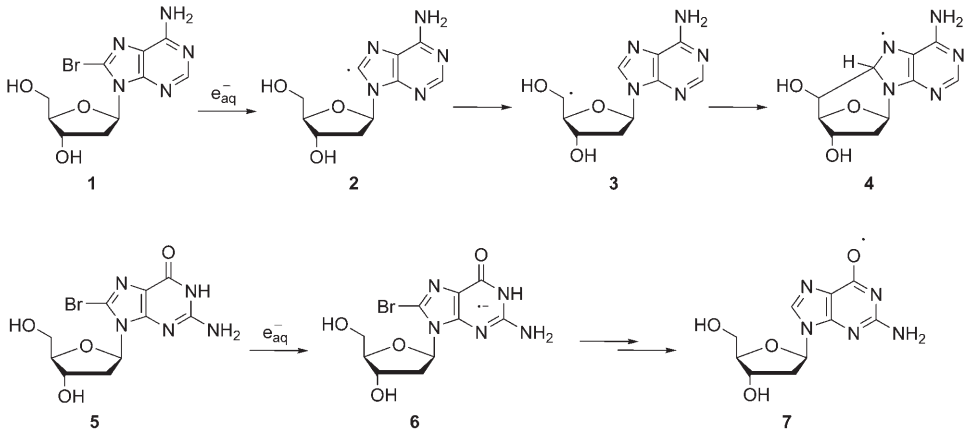

Scheme 1. Chemical studies of hydrated electrons with 8-bromo-2′-deoxyadenosine (**1**) and 8-bromo-2′-deoxyguanosine (**5**) show two different reaction paths.

light-dependent flavin electron injector in the loop region of the hairpin were found to capture electrons with quantitative formation of the corresponding debrominated oligonucleotides, as do the analogous 8-bromo-2′-deoxyguanosine derivatives.[10] In G quadruplexes, the reaction with e_{aq}^- indicated, for the first time, that excess electron transfer is also effective in this supramolecular arrangement.[9]

In the present work, we extended our studies to 8-bromohypoxanthine nucleosides. In particular, 8-bromo-2′-deoxyinosine (**8**) and 8-bromoinosine (**12**) have been investigated by using radiolytic methods coupled with product studies. Furthermore, BB1K-HMDFT calculations were carried out on radical anions of 8-bromo-9-methyl purines in order to understand the influence of heteroaromatic rings.

Results and Discussion

Synthesis and acid–base properties of 8-bromo-2′-deoxyinosine (8): Compound **8** was prepared by using the procedure of Holmes and Robins for the synthesis of 8-bromoinosine,[12] although some experimental conditions were changed in order to improve the yield. Briefly, a suspension of the corresponding adenine derivative **1** in acetic acid was treated with sodium nitrite. After basic workup, the residue was purified by using reverse-phase silica gel chromatography followed by recrystallization to give pure **8** in a 30% overall yield.

At pH ≈ 7, the UV spectrum of **8** exhibits two bands at $\lambda \approx 210$ and 255 nm that are typical of other purine nucleosides, with a molar absorption coefficient (ε) of $1.35\times10^4\,\text{M}^{-1}\text{cm}^{-1}$ at 255 nm. The spectrum showed a pH dependence, and a pK_a value of 8.7 was obtained from the analysis of the optical density versus pH curves. A similar experiment performed for 2′-deoxyinosine and inosine gave pK_a values of 9.2[13] and 8.8, respectively.[14] For comparison, a pK_a of 8.4 has been reported for 8-bromoguanosine,[4] whereas pK_a values for the related debrominated derivatives have been found to be substantially higher, for example, 9.40 for 2′-deoxyguanosine[15a] and 9.25 for guanosine.[15] Therefore, the acid–base properties of the purine moiety appear to be influenced by the electron-withdrawing bromine atom at the C8 position.

Reaction of hydrated electrons (e_{aq}^-) with 8 and 12: Radiolysis of neutral water leads to e_{aq}^-, HO•, and H•, as shown in Equation (1). The values in parentheses represent the radiation chemical yields (G) in $\mu\text{mol J}^{-1}$.[16a] The reactions of e_{aq}^- with the substrates were studied in deoxygenated solutions containing 0.25 M *t*BuOH. As the rate constants of HO• radical[16] and H• atoms[17] with *t*BuOH [Eq. (2)] are 6.0×10^8 and $1.2\times10^6\,\text{M}^{-1}\text{s}^{-1}$, respectively, the substrate concentration was chosen so that the majority of the HO• and H• species are scavenged by *t*BuOH.[18]

$$H_2O \xrightarrow{\text{radiolysis}} e_{aq}^- \ (0.27),\ HO^\bullet \ (0.28),\ H^\bullet \ (0.062) \qquad (1)$$

$$HO^\bullet/H^\bullet + t\text{BuOH} \rightarrow (CH_3)_2C(OH)CH_2^\bullet + H_2O/H_2 \qquad (2)$$

The rate constants for the reaction of e_{aq}^- with **8** or **12** were determined to be $(1.6\pm0.1)\times10^{10}$ and $(1.7\pm0.1)\times10^{10}\,\text{M}^{-1}\text{s}^{-1}$, respectively, by measuring the rate of the optical density decrease of e_{aq}^- at $\lambda = 720$ nm ($\varepsilon = 1.9\times10^4\,\text{M}^{-1}\text{cm}^{-1}$)[19] as a function of the nucleoside concentration (see the Supporting Information). These values are very similar to the analogous reactions with 8-bromoadenine[2,3] and 8-bromoguanine[4,6] nucleosides.

The reaction of an aqueous solution of **8** (1 mM) and *t*BuOH (0.25 M) at pH ≈ 7 with e_{aq}^- in the absence of O_2 was complete within ≈300 ns. At this time, no significant absorption was detected in the $\lambda = 300$–700 nm region. However, a spectrum containing three bands centered at 310, 350, and 500 nm developed in ≈20 μs (Figure 1). The time profile for the formation of the transient at $\lambda_{max} = 350$ nm (inset a) followed first-order kinetics with a rate constant that was independent of [**8**] in the concentration range 0.1–1 mM and which slightly increased with the dose/pulse ratio. This dose dependence is attributed to the mixing of first-order growth and second-order decay of the species. Extrapolation to zero dose gave a rate constant of $k_c = (1.4\pm0.1)\times10^5\,\text{s}^{-1}$ at 20 °C. Inset b shows the effect of the dose on the apparent molar absorption coefficient at 350 nm (ε_{app}), calculated by assuming a radiation chemical yield of 0.27 $\mu\text{mol J}^{-1}$, which is the G of hydrated electrons.[16a] A molar absorption coefficient of $5000\pm100\,\text{M}^{-1}\text{cm}^{-1}$ at 350 nm was calculated by extrapolating to zero dose.

In analogy to the reaction of 8-bromo-2′-deoxyadenosine **1**,[2] we assigned the transient shown in Figure 1 to the con-

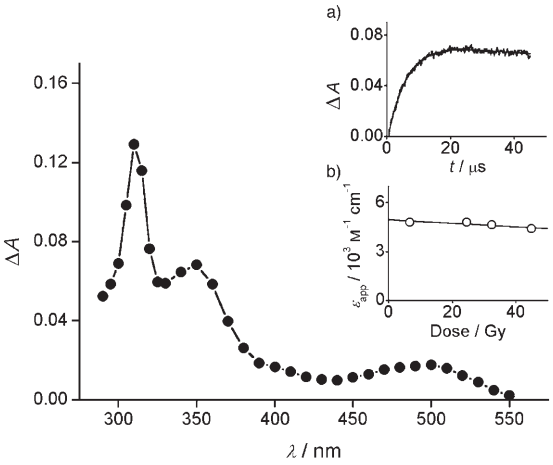

Figure 1. Transient absorption spectrum obtained from the pulse radiolysis of an Ar-purged solution containing **8** (1 mM) and *t*BuOH (0.25 M) at pH ≈ 7, taken 20 μs after the pulse; dose = 25.5 Gy, optical path = 2.0 cm. Insets: a) Time-dependence of the absorption at $\lambda = 350$ nm; the solid line represents the first-order kinetic fit to the data; b) Dependence of ε_{app} (see text) at $\lambda = 350$ nm on the radiation dose.

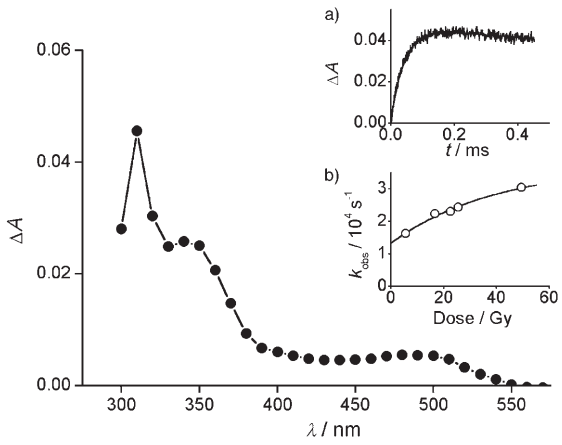

Figure 2. Transient absorption spectrum obtained from the pulse radiolysis of an Ar-purged solution containing **12** (1 mM) and *t*BuOH (0.25 M) at pH ≈ 7, taken 170 μs after the pulse; dose = 23.8 Gy, optical path = 2.0 cm. Insets: a) Time-dependence of absorption at $\lambda = 310$ nm; dose = 22.6 Gy; b) Dependence of k_{obs} (see text) from the radiation dose at $\lambda = 310$ nm.

jugated aminyl radical **11** and the observed first-order growth to the cyclization of radical **10** (Scheme 2).

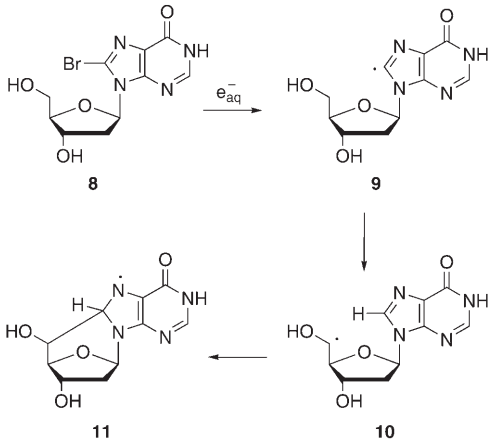

Scheme 2. Proposed mechanism for the reaction of hydrated electrons with 8-bromo-2′-deoxyinosine (**8**).

Under the same conditions, the reaction of e_{aq}^- with **12** gave a similar spectrum that developed more slowly, namely 170 μs (Figure 2). The time profile for the formation of the transient at $\lambda_{max} = 310$ nm (Figure 2, inset a) follows first-order kinetics with a rate constant (k_{obs}) that is independent of **12** in the concentration range 0.2–1 mM. As expected from the mixing of the first-order growth and the second-order decay, k_{obs} increased with the dose/pulse ratio (Figure 2, inset b). An empirical expression was used to fit the experimental data and extrapolate to zero dose[20] to give a rate constant of $k_c = (1.3 \pm 0.1) \times 10^4\ s^{-1}$ at 20 °C. The absorbance at $\lambda = 310$ nm is also found to vary substantially with the dose. An apparent extinction coefficient (ε_{app}) of $5900 \pm 100\ M^{-1}cm^{-1}$ at 310 nm was calculated by extrapolating to zero dose and assuming $G = 0.27\ \mu mol\ J^{-1}$.

In analogy to the reaction of the 2′-deoxyribo derivative **8**, we assigned the transient in Figure 2 to the conjugated aminyl radical **15**, and the observed rate to the cyclization of radical **14** (Scheme 3).

A comparison of the reactions of e_{aq}^- with **8** and **12** shows that the transient spectra are developed in 20 and 170 μs, respectively, and accordingly, the cyclization rate constant for the reaction **10**→**11** is 11 times faster than that of the reaction **14**→**15**. This is probably a consequence of the conformational changes between ribo and 2′-deoxyribo derivatives.

Figure 3 compares the spectra of aminyl radicals **11** (●) and **15** (▲). The absorbance at the maxima (310 and 350 nm) of the two species are quite different: one being 60 % of the other. The shape of both spectra strongly resemble that assigned to the isostructural radical **19** (▽), obtained from the reaction of inosine with H• atoms.[14] However, the unexpected similarities of reported ε values for **19** and our radical **15** forced us to reinvestigate the reaction of inosine with H• atoms.

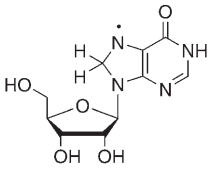

19

The reaction of an N_2O-saturated aqueous solution of inosine (2 mM) and *t*BuOH (0.2 M) at pH ≈ 7 afforded the spectrum (◇) shown in Figure 3, which has an ε value 60–70 % higher than that reported in the literature.[14] The similarities in shape and ε values between radical **11** (●) and **19** (◇) are gratifying. Therefore, the difference in ε values between radical **11** and **15** suggests that only ≈ 60 % of the radicals produced by the reaction of the hydrated electron with **12** leads to radical **15** (Scheme 3).

More information on the reaction of e_{aq}^- with **12** was obtained by experiments in the presence of *N*,*N*,*N*′,*N*′-tetra-

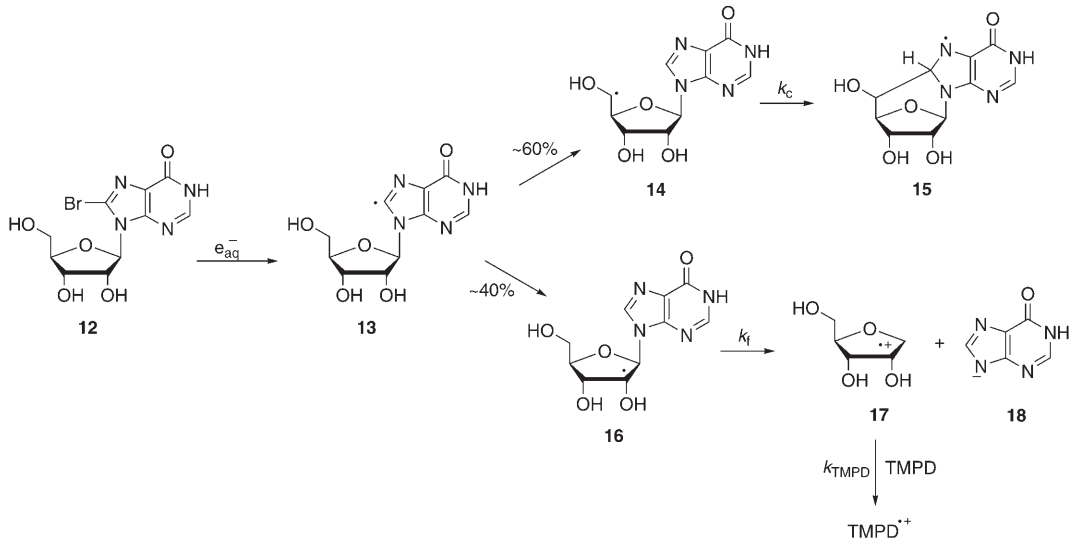

Scheme 3. Proposed mechanism for the reaction of hydrated electrons with 8-bromoinosine (**12**).

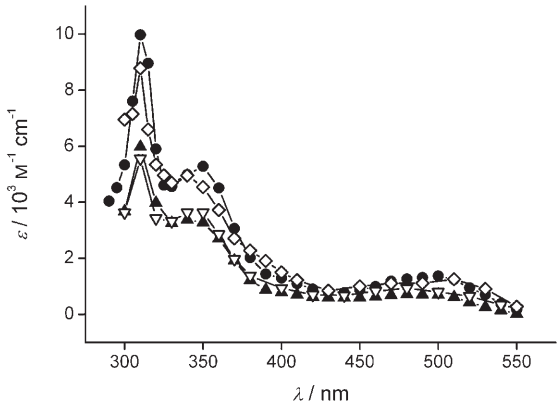

Figure 3. Transient absorption spectra obtained from the pulse radiolysis of solutions containing (●) **8** (1 mM) and *t*BuOH (0.25 M) at pH ≈ 7, Ar-purged, taken 20 μs after the pulse, assuming $G = 0.27$ μmol J^{-1} and extrapolating to zero dose; (▲) **12** (1 mM) and *t*BuOH (0.25 M) at pH ≈ 7, Ar-purged, taken 170 μs after the pulse, assuming $G = 0.27$ μmol J^{-1} and extrapolating to zero dose; (▽) taken from ref. [14] and refers to inosine (0.2 mM) and *t*BuOH (0.1 M) at pH ≈ 7, N_2O-saturated, taken 40 μs after the pulse; (◇) inosine (2 mM) and *t*BuOH (0.2 M) at pH ≈ 7, N_2O-saturated, taken 9 μs after the pulse, dose = 19.6 Gy, assuming $G = 0.084$ μmol J^{-1}.

methyl-*p*-phenylenediamine (TMPD, E°(TMPD$^{\bullet+}$/TMPD) = 0.27 V),[21] as previously reported for the case of 8-bromoadenosine.[3] Pulsing O_2-free aqueous solutions of **12** (1 mM) containing *t*BuOH (0.25 M) and different concentrations of TMPD (30–120 μM) at pH ≈ 7 led to the oxidation of TMPD. The rate constants for this oxidation and the associated formation of TMPD$^{\bullet+}$ were measured at $\lambda = 565$ nm ($\varepsilon = 1.25 \times 10^4$ M^{-1} cm^{-1}), which represents one of the absorption maxima of TMPD$^{\bullet+}$ (see the Supporting Information).[22,23] Because HO$^{\bullet}$ radicals are trapped by *t*BuOH under these experimental conditions and the reaction of TMPD with the carbon-centered radicals derived from *t*BuOH is unimportant on the timescale of our experiments,[24] we concluded that the TMPD$^{\bullet+}$ radical cation is formed from intermediates generated by the reaction of e_{aq}^- with **12**.[25]

The yield of TMPD$^{\bullet+}$ (corrected for its decay) increased on increasing the TMPD concentration, varying between 17% for [TMPD] = 30 μM to 35% for [TMPD] = 120 μM, with respect to the yield of e_{aq}^-. The induction period observed for the formation of TMPD$^{\bullet+}$ was satisfactorily fitted with a two consecutive reaction model. The first component is independent of TMPD concentration and occurs with a rate constant of $k_f \approx 7 \times 10^4$ s^{-1}. The second component depends on the concentration of TMPD, and the rate constant $k_{TMPD} \approx 2 \times 10^8$ M^{-1} s^{-1} is assigned to the species reacting with TMPD. We suggest that the initially produced radical **13** partitioned its translocation step between two channels to afford the C5′-radical **14** and the C2′-radical **16** (Scheme 3), similar to the case of 8-bromoadenosine.[3] The rate constant for heterolytic cleavage of the glycosidic bond, which produces the radical cation **17** and hypoxanthine **18**, is slightly smaller than the analogous reaction of the 2′-adenosinyl radical ($k_f = 1.1 \times 10^5$ s^{-1}).[3] Radical cation **17** oxidizes TMPD with a rate constant of $k_{TMPD} \approx 2 \times 10^8$ M^{-1} s^{-1}.

Redox properties of radicals 10 and 11: Next we investigated the reactivity of the C5′ radical **10** and aminyl radical **11** with respect to $[Fe(CN)_6]^{3-}$, methyl viologen (MV^{2+}), and molecular oxygen in analogy to the reactions observed for radicals **3** and **4**.[2]

In the case of $[Fe(CN)_6]^{3-}$, for which $E^{\circ}([Fe(CN)_6]^{3-}/[Fe(CN)_6]^{4-}) = 0.36$ V,[21a,26] this was tested by submitting deaerated solutions of **8** (1 mM) containing *t*BuOH (0.25 M) and different concentrations of $K_3[Fe(CN)_6]$ (25–100 μM) at pH 7 to pulse radiolysis. Under these conditions, e_{aq}^- reacts exclusively with **8**, as $k(e_{aq}^- + [Fe(CN)_6]^{3-}) = 3.1 \times 10^9$ M^{-1} s^{-1}.[16] The absorption at $\lambda = 350$ nm was found to decrease by increasing the concentration of $[Fe(CN)_6]^{3-}$ (see inset of Figure 4). A Stern–Volmer type of approach gave

$k_{ox}(\mathbf{10}/[Fe(CN)_6]^{3-})/k_c = 1.5\times10^4\,M^{-1}$ (Figure 4). Combination of this data with the k_c value yielded $k_{ox}(\mathbf{10}/[Fe(CN)_6]^{3-}) = (2.0\pm0.3)\times10^9\,M^{-1}s^{-1}$, which is attributed to a reaction of the C5′ radical **10** with $[Fe(CN)_6]^{3-}$ to afford the corresponding cation.

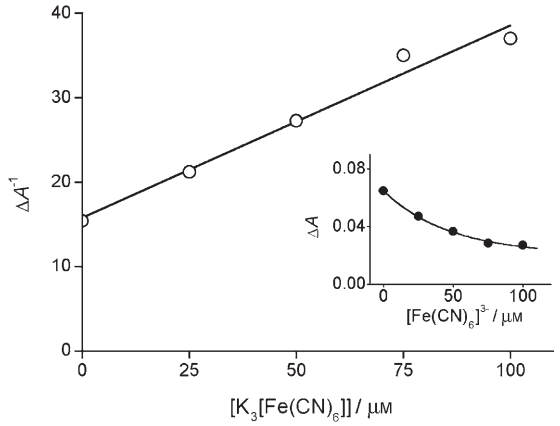

Figure 4. Dependence of $1/\Delta A$ at $\lambda = 350$ nm on $[K_3[Fe(CN)_6]]$ obtained from the pulse radiolysis of Ar-purged solutions containing **8** (1 mM) and *t*BuOH (0.25 M) at pH ≈ 7; optical path = 2.0 cm, dose = 24.6 Gy. Inset: Dependence of ΔA at $\lambda = 350$ nm on $[K_3[Fe(CN)_6]]$. The solid line represents an exponential fit to the data.

On the other hand, the decay of the transient at 350 nm followed first-order kinetics in the presence of $[Fe(CN)_6]^{3-}$ (see inset of Figure 5). From the slope of $k_d(\mathbf{11})$ versus $[K_3[Fe(CN)_6]]$, the bimolecular rate constant was found to be $k_{ox}(\mathbf{11}/[Fe(CN)_6]^{3-}) = (8.9\pm0.2)\times10^8\,M^{-1}s^{-1}$ (Figure 5), indicating that $[Fe(CN)_6]^{3-}$ efficiently oxidizes the aromatic aminyl radical **11**.

The reactivity of the transient species towards the weaker oxidant methyl viologen (MV^{2+}), for which $E^{\circ}(MV^{2+}/MV^{\bullet+}) = -0.45$ V,[21] was also investigated. The experiments were performed by adding different concentrations of MV^{2+} (50, 100, or 150 μM) to Ar-purged solutions containing **8** (1 mM) and *t*BuOH (0.25 M). Under these conditions, **8** and MV^{2+} should compete for e_{aq}^- because $k(e_{aq}^- + MV^{2+}) = 7.2\times10^{10}\,M^{-1}s^{-1}$.[16] Indeed, a two-component increase of the absorption at $\lambda = 605$ nm, characteristic of the methyl viologen radical cation ($MV^{\bullet+}$, $\varepsilon_{605\,nm} = 1.37\times10^4\,M^{-1}cm^{-1}$),[27] was observed upon irradiation. For example, using 100 μM MV^{2+}, the instantaneous formation of $MV^{\bullet+}$ accounted for 29% of e_{aq}^-, whereas the slow growth accounted for 8.5%. As the $Me_2C(OH)CH_2^{\bullet}$ radical does not react with MV^{2+}, this demonstrated an electron transfer between the precursor of the aminyl radical (i.e., C5′ radical **10**) and MV^{2+} with a rate constant of $k_{ox}(\mathbf{10}/MV^{2+}) = (2.0\pm0.6)\times10^8\,M^{-1}s^{-1}$. It is also worth mentioning that, under these conditions, the $MV^{\bullet+}$ decays by second-order kinetics ($k_d = 3.1\times10^9\,M^{-1}s^{-1}$), which probably involves a back-electron transfer to the aminyl (**11**) or to the $Me_2C(OH)CH_2^{\bullet}$ radical.

The reactivity towards molecular oxygen was investigated by pulsing solutions of **8** (1 mM) containing *t*BuOH (0.25 M) and different concentrations of O_2 (0–140 μM) at pH 7. The absorption at 350 nm was found to decrease on increasing the O_2 concentration (Figure 6). This decrease could be attributed to the reactions of e_{aq}^- with **8** and O_2 because $k(e_{aq}^- + O_2) = 1.9\times10^{10}\,M^{-1}s^{-1}$.[16] Taking into consideration the percentage of e_{aq}^- captured by O_2 and the use of a Stern–Volmer type of approach (Figure 6, inset a), we obtained $k_{ox}(\mathbf{10}/O_2)/k_c = 8.8\times10^3\,M^{-1}$. Combination of this data with the k_c value yielded $k_{ox}(\mathbf{10}/O_2) = (1.2\pm0.4)\times10^9\,M^{-1}s^{-1}$. On the other hand, the first-order growth (k_{obs}) increased linearly by increasing the oxygen concentration, that is, $k_{obs} = k_c + k_{ox}(\mathbf{10}/O_2)\times[O_2]$. From the slope of k_{obs} versus $[O_2]$, the bimolecular rate constant was found to be $k_{ox}(\mathbf{10}/O_2) = (2.7\pm0.1)\times10^9\,M^{-1}s^{-1}$ (inset b). An average value of $k_{ox}(\mathbf{10}/O_2) =$

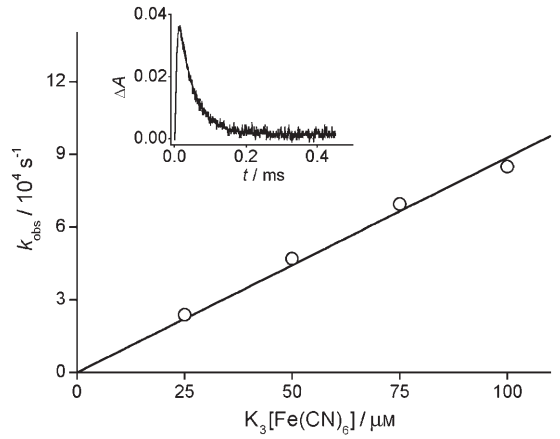

Figure 5. Dependence of k_{obs} for decay at $\lambda = 350$ nm on $[K_3[Fe(CN)_6]]$ obtained from the pulse radiolysis of Ar-purged solutions containing **8** (1 mM) and *t*BuOH (0.25 M) at pH ≈ 7. Inset: Time-dependence of the absorption at 350 nm in the presence of $K_3[Fe(CN)_6]$ (25 μM); optical path = 2.0 cm, dose = 23.9 Gy. The solid line represents the first-order kinetic fit to the data.

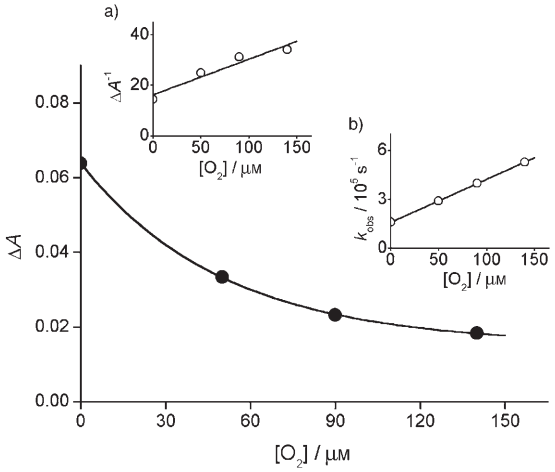

Figure 6. Dependence of ΔA at $\lambda = 350$ nm on $[O_2]$ obtained from the pulse radiolysis of solutions containing **8** (1 mM) and *t*BuOH (0.25 M) at pH ≈ 7 saturated with Ar/O_2 mixtures; optical path = 2.0 cm, dose = 22.5 Gy. The solid line represents an exponential fit to the data. Insets: a) Dependence of ΔA^{-1} at 350 nm on $[O_2]$; b) Dependence of k_{obs} for growth at 350 nm on $[O_2]$.

$(2\pm1)\times10^9\,\text{M}^{-1}\text{s}^{-1}$ is suggested for the reaction of the C5′ radical **10** with molecular oxygen.

The presence of O_2 also influenced the disappearance of radical **11**. The second-order (SO) kinetics became faster as the concentration of O_2 increased. Figure 7 shows the dependence of $k(SO)_{obs}$ on $[O_2]$, and its inset shows the second-order kinetic fit to the data for 50 μM of oxygen. Such behavior is consistent with the reversible reaction of aminyl radical **11** with O_2 to give the corresponding peroxyl adduct [Eq. (3/−3)], followed by cross-termination between this radical and a second radical **11** [Eq. (4)]. Under these conditions, the second-order rate constant, $k(SO)_{obs}$, will be a complex function of $[O_2]$, k_3, k_{-3}, and k_4.[28]

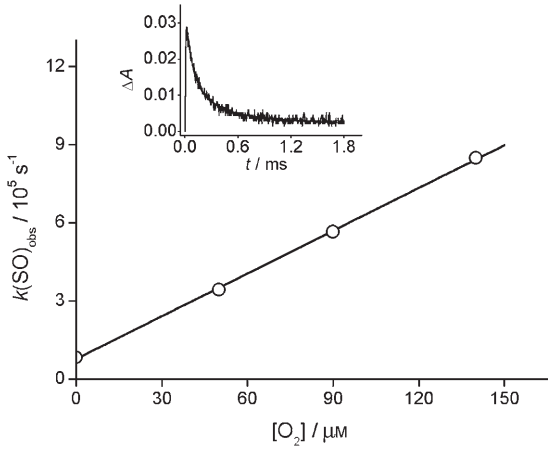

Figure 7. Dependence of k_{obs} for second-order decay at $\lambda=350$ nm on $[O_2]$ obtained from the pulse radiolysis of solutions containing **8** (1 mM) and *t*BuOH (0.25 M) at pH ≈ 7 saturated with Ar/O_2 mixtures. Inset: Time-dependence of absorption at 350 nm in the presence of 50 μM O_2; optical path = 2.0 cm, dose = 20.9 Gy. The solid line represents a second-order kinetic fit to the data.

$$\mathbf{11}^{\cdot} + O_2 \rightleftharpoons \mathbf{11}\text{-}OO^{\cdot} \qquad (3/-3)$$

$$\mathbf{11}\text{-}OO^{\cdot} + \mathbf{11}^{\cdot} \rightarrow \text{products} \qquad (4)$$

Table 1 summarizes the results obtained for the oxidation of C5′ radicals **3** and **10**. The reactivities of the two species are very similar. The rate constants for the reactions with oxygen are typical for α-heteroatom-substituted alkyl radicals.[16,29,30] The rate constants for the reactions with MV^{2+} are at least one order of magnitude slower than those with the stronger oxidant $[Fe(CN)_6]^{3-}$, which probably involve an inner-sphere electron-transfer process.[31]

Table 1. Rate constants for the oxidation of C5′ radicals.

Oxidizing agent	k_{ox} of radical **3**[a,b] [$\text{M}^{-1}\text{s}^{-1}$]	k_{ox} of radical **10**[a] [$\text{M}^{-1}\text{s}^{-1}$]
oxygen	$(1.8\pm1)\times10^9$	$(2\pm1)\times10^9$
$[Fe(CN)_6]^{3-}$	$(4.2\pm0.4)\times10^9$	$(2.0\pm0.3)\times10^9$
MV^{2+}	$(2.2\pm0.4)\times10^8$	$(2.0\pm0.6)\times10^8$

[a] Reactions in neutral water at 22 ± 2 °C. [b] Data from ref. [2].

Product studies from continuous radiolysis of 8 and 12: Deaerated samples of an aqueous solution of **8** (≈1.5 mM) and *t*BuOH (0.25 M) at pH ≈ 7, were irradiated under steady-state conditions with a total dose of 2.0 kGy at a dose rate of ≈13 Gy min^{-1}. HPLC analysis of the reaction showed complex unresolved mixtures. Repetition of the experiment in the presence of $K_4[Fe(CN)_6]$ (4 mM) gave different results.[32] HPLC analysis showed that 34% of the starting bromide was consumed and that a few products were formed. The compounds (5′*R*)-5′,8-cyclo-2′-deoxyinosine (**21**) and (5′*S*)-5′,8-cyclo-2′-deoxyinosine (**23**) were identified by comparison with authentic samples (see below), the major compound being the 5′*R* isomer in a 64% yield (based on the reacted bromide). Hypoxanthine (**25**) and 2′-deoxyinosine (**26**) were also identified as minor products by comparison with commercially available compounds, whereas hydrated 5′-carboxaldehyde-2′-deoxyinosine (**24**) is tentatively assigned on the basis of LC–MS analysis. Interestingly, the ratio (5′*R*)/(5′*S*) ≈ 6:1 was very similar to that reported for the analogous experiments with 8-bromo-2′-deoxyadenosine.[2]

Scheme 4 shows the proposed reaction mechanism. The cyclization of the C5′ radical affords aminyl radicals **20** and **22** with a defined stereochemistry at the C5′ and C8 positions with the new six-membered ring being in the chair

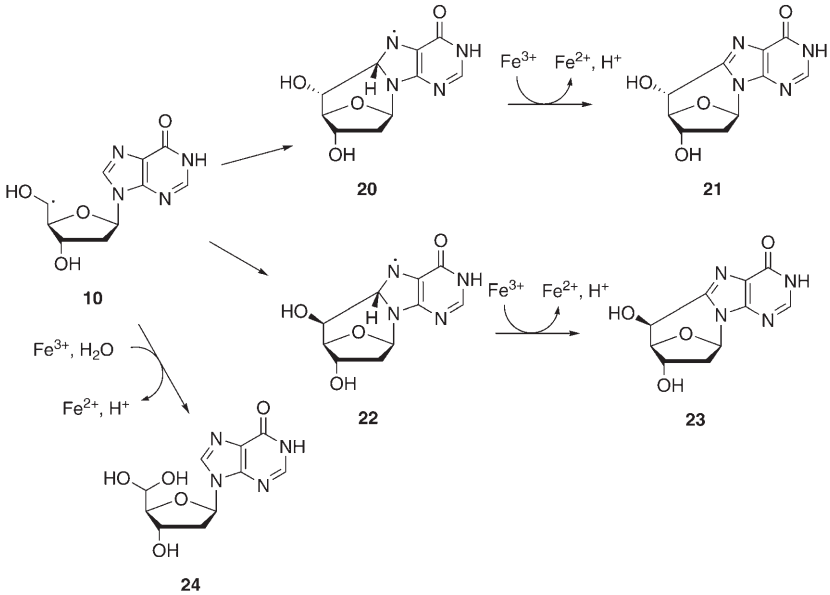

Scheme 4. Proposed mechanism for the formation of nucleosides derived from C5′ radical **10**.

conformation. Radicals **20** and **22** are readily oxidized by $[Fe(CN)_6]^{3-}$ to products **21** and **23**. Hydrated aldehyde **24** should be derived from the oxidation of radical **10**. The minor amounts of **26** could be explained by reduction of radicals **9** or **10**; alternatively, a H$^{\bullet}$ might add to the C8=N7 double bond of **8**. The release mechanism of base **25** may involve minor paths of radical translocation of intermediate **9** to positions other than the C5′ of the sugar moiety (Scheme 2).

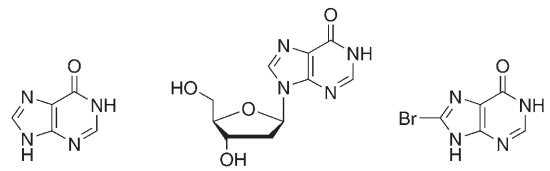

25 **26** **27**

Deaerated aqueous solutions of **12** (≈1.5 mM) and *t*BuOH (0.25 M) at pH≈7 were irradiated under stationary-state conditions with a total dose of up to 2.0 kGy at a dose rate of ≈12 Gy min^{-1}, followed by HPLC and LC–MS analyses. The main reaction product was hypoxanthine (**25**), which accounts for ≈20% of the reacted bromide. These results are in good agreement with the aforementioned pulse radiolysis observations. It is worth mentioning that **25** was a minor reaction product in the analogous experiment with **8**, which further supports our conclusion that the free base may be derived by C2′ radical chemistry.

Steady-state photolysis studies of 8: Bromide **8** was irradiated with UV light under a variety of experimental conditions. The crude reaction mixtures were analyzed by means of HPLC coupled with UV (diode array) and MS (ion trap) detection, using authentic samples as reference compounds for identification. Table 2 and Scheme 4 summarize the experimental findings and the reaction products. The yields are based on the consumption of the starting bromide for a better comparison. Workup of the reaction in entry 3 allowed the isolation and characterization of the two diastereoisomers **21** and **23**. Support for the correct configuration assignment at the C5′ position was provided by ^{1}H NMR analyses and, in particular, by the magnitude of J(H4′,H5′).

Table 2. Yields of products obtained by UV photolysis of deaerated solutions of **8**.[a]

Entry	Solvent	Conditions		Conv.	Product yields [%]					
		t [h]	pH	[%]	**21**	**23**	**24**	**25**	**26**	**27**
1	H_2O	3	7→4[b]	35	30	8	13	<5	11	28
2	H_2O	3	7[c]	25	31	<1	17	13	31	–
3	H_2O/NaI[d]	1.5	7→4[b]	91	38	10	26	10	3	8

[a] Irradiation of **8** (10 mL per tube, 1 mM) under N_2 was performed with a multilamp photoreactor at λ=254 nm. Yields are based on the conversion of bromide **8**. Estimated errors are less than 10% of the stated values. [b] pH changed during the course of the reaction. [c] Buffer solution with KH_2PO_4/Na_2HPO_4 (10 mM). [d] Solution of **8** with 2 mM NaI.

For one isomer, the coupling constant J(H4′,H5′) is 0.6 Hz (in DMSO), which is indicative of a dihedral angle of ≈90° between these two protons and is compatible with 5′*R* stereoconfiguration. The 5′*S* isomer has J(H4′,H5′)=6.9 Hz. These findings are in very good agreement with ^{1}H NMR data of other 5′,6-cyclopurine derivatives.[2,33]

Entry 1 in Table 2 shows the reaction in an aqueous medium and at natural pH. After 3 h of photolysis, the cyclic products (**21** and **23**) were formed in a 38% overall yield and in a ratio (5′*R*)/(5′*S*)=3.9, together with a 13% yield of hydrated 5′-carboxaldehyde (**24**). The reduced product (**26**) was also formed. As was reported for the analogous adenine derivative **1**, N-glycosidic bond hydrolysis is favored at acidic pH values[7] and leads to **27**. This pathway was inhibited in a buffered solution at pH 7 (entry 2).

To test the ability of halide anions (I^-) to trap Br$^{\bullet}$ atoms in the photolysis mixture, the reaction was carried out in water in the presence of NaI to generate $IBr^{-\bullet}$.[7] Entry 3 in Table 2 shows the results of photolysis of a deaerated aqueous solution containing 1 mM of **8** in the presence of 2 equiv of NaI. A much higher conversion rate (91% relative to 35% in water) was observed, although the diastereomeric ratio between the cyclic photoproducts **21** and **23** was maintained. Therefore, the equilibrium $Br^{\bullet}+I^- \rightleftharpoons BrI^{\bullet-}$ plays an important role in this synthetically useful radical cascade by regulating the relative concentrations of the two reactive oxidizing species.[7]

All these results support the mechanism shown in Scheme 4 in which the formation of radical C5′ is followed by different reaction pathways. Among the oxidized products, formation of 5′,8-cyclopurines **21** and **23** competes with that of the hydrated aldehyde **24** as the main processes.

The origin of differences in behavior between 8-bromopurine nucleosides: The radical anions of 8-bromohypoxanthine derivatives are not stable and lose Br^- to form the neutral σ-type radical at C8, as found experimentally for the radical anion of 8-bromoadenine derivatives. On the other hand, radical anions of 8-bromoguanine derivatives have been found to be stable and undergo very fast protonation. BB1K-HMDFT calculations were carried out on 8-bromo-9-methyladenine (**28**), 8-bromo-9-methylguanine (**29**), and 8-bromo-9-methylhypoxanthine (**30**) to understand this different behavior.

At this level of theory, the radical anion of **28** is computed to be unstable, as found previously for 8-bromo-2′-deoxyadenosine with B3LYP-HDFT calculations.[3] On the contrary, radical anions of **29** and **30** are stable. The C8–Br bond length increases only slightly on going from the neutral molecule to the radical anion, namely, from 1.845 to 1.864 Å for **29** and from 1.844 to 1.864 Å for **30**, as expected for a delocalized π-radical anion. As the C–Br bond elongates, these radical anions remain planar and their energy increases. However, the energy gap decreases between the π*-radical anion and the σ*-radical anion, where the unpaired electron is located at the $\sigma^*_{C8\text{-}Br}$ antibonding MO, until, at a large C–Br distance, the σ*-anionic state becomes more stable than

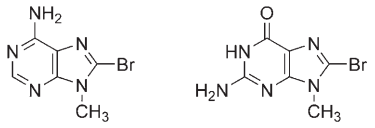

28 29

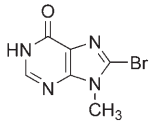

30

the π*-anionic state. At a larger C8–Br distance, the C8 site becomes strongly pyramidal and the energy of the radical anions decreases rapidly so that they tend to lose Br^-. Interestingly, crossover between the two states occurs at a shorter C8–Br bond length for the radical anion of **30** (2.01 Å) than for the radical anion of **29** (2.095 Å). This indicates that cleavage of the C–Br bond should be easier in the 8-bromohypoxanthine derivatives than in 8-bromoguanine analogues during pulse radiolysis experiments. Indeed, the energy increase caused by the elongation of the C–Br bond at the crossing point is small (15.9 kJ mol^{-1}) for the radical anion of **30**, whereas it is significant (35.2 kJ mol^{-1}) for the radical anion of **29**. This different behavior can be rationalized on the basis of the electron distribution in the LUMO of **28**, **29**, and **30**, namely, in the MO where the extra electron is captured.

Figure 8 shows that in the LUMO of **28** (**A**) the electron density is largely localized at C8 (22.1%), which is the carbon linked to the Br atom. A significant electron density is also computed at the Br atom (4.1%). Hence the unpaired electron in the anion tends to occupy the antibonding $\sigma^*_{C8\text{-}Br}$ MO upon relaxation of the structural parameters

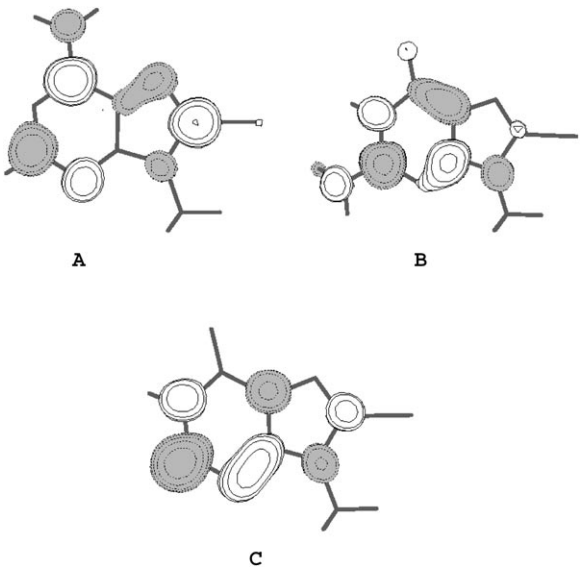

Figure 8. LUMO of derivatives **28** (**A**), **29** (**B**), and **30** (**C**) computed at the BB1K-HMDFT level.

thus favoring the loss of Br^-. The electron densities at the C8 (7.5%) and Br (1.2%) atoms decrease significantly in the LUMO of **30** (**C**) so that the π-radical anion state is slightly more stable than the σ-radical anion state. This explains the small value computed for the C–Br dissociation barrier. In the LUMO of **29** (**B**), the electron density becomes negligible (2.3% at C8 and 0.3% at Br) so that the π-radical anion state is significantly more stable than the σ-radical anion state. The C–Br dissociation barrier increases and the lifetime of the π-radical anions is now sufficient to be protonated at C8, as occurs in the unsubstituted 2′-deoxyadenosine and 2′-deoxyguanosine.[34] Figure 8 shows that there is a shift of electron density from the five-membered ring to the six-membered ring on going from **28** to **30** and from **30** to **29**. The electronic distribution in the LUMO of **28** is delocalized over the two rings. Substitution of a π-electron-releasing amino group in the six-membered ring with a π-electron-withdrawing carbonyl group in the LUMO of **30** tends to enhance the extra electron delocalization in the six-membered ring. In the LUMO of **29**, the extra electron is mainly localized on the six-membered ring owing to the adjunctive presence of a carbon atom (C2) that is extremely electron deficient in the neutral molecule, because it is surrounded by three electronegative atoms.

Conclusion

The results described herein demonstrate that the reaction of **8** with e_{aq}^- at pH≈7 leads to a C5′ radical **10**, whereas the analogous reaction with 8-bromoinosine **12** with e_{aq}^- at pH≈7 leads to C5′ radical **14** and C2′ radical **16** in a ratio of ≈60:40. We found that the C5′ radical adds intramolecularly to the C8=N7 double bond in the hypoxanthine moiety with rate constants of 1.4×10^5 and 1.3×10^4 s^{-1} for the 2′-deoxyribo and ribo forms, respectively, affording the 5′*R* and 5′*S* isomers. The C2′ radical liberates hypoxanthine with a rate constant of 7×10^4 s^{-1}. Redox properties of radicals **10** and **11** have also been obtained. The similarities between 8-bromohypoxanthine and 8-bromoadenine[2,3] derivatives towards e_{aq}^- and the differences between 8-bromohypoxanthine and 8-bromoguanine[4,5] derivatives towards e_{aq}^- can be rationalized in terms of the energy gap between the π*-radical anion and the σ*-radical anion by means of BB1K-HMDFT calculations. We took advantage of the observed chemical behavior to develop a synthetically useful photoreaction that converts **8** into (5′*R*)-5′,8-cyclo-2′-deoxyinosine (**21**) and (5′*S*)-5′,8-cyclo-2′-deoxyinosine (**23**) in a ratio of 4:1 and in a one-pot procedure. Our findings extend the observations of a different radical reactivity between 2′-deoxyribo and ribo nucleosides, and provide a molecular basis for forthcoming experiments with model DNA or RNA radicals to elucidate biological damage. Moreover, the radical reactivity of hypoxanthine derivatives may be useful for studies concerning nucleoside-type natural products, which are interesting for developing drugs, and in other pharmacological studies.[35]

Experimental Section

Chemicals: 8-Bromo-2′-deoxyadenosine was provided by Berry & Associates (Ann Arbor, MI, USA). 8-Bromoinosine, sodium iodide, $K_4[Fe(CN)_6]$, and the phosphate buffer were purchased from Sigma-Aldrich. Acetonitrile and methanol, both HPLC grade, were from Scharlau. Water was purified through a Millipore Milli-RO plus 30 system.

Instrumentation: Reverse-phase HPLC analysis was performed on a Waters apparatus equipped with a Agilent column (SB-Zorbax, 150×4.6 mm, 5 μm), a Waters 2996 photodiode array detector at fixed wavelength of 254 nm and a Waters 600 controller. The chromatographic system used for analytical experiments consisted of acetonitrile and water as eluents [linear gradient from 0 to 5% of acetonitrile (30 min), from 5% to 15% of acetonitrile (50 min), 5 min at 15:85 (CH_3CN/H_2O) and from 15% to 0% of acetonitrile (60 min)] at a flow rate of 0.7 mL min^{-1}.

Pulse radiolysis: Pulse radiolysis with optical absorption detection was performed on the 12 MeV linear accelerator, which delivered 20–200 ns electron pulses with doses between 5 and 50 Gy. This generated $HO^{\bullet}$, $H^{\bullet}$, and e_{aq}^- in concentrations of 1–20 μM. The pulse irradiations were performed at room temperature (22±2°C) on samples contained in Spectrosil quartz cells of 2 cm optical path length. Solutions were protected from the analyzing light by means of a shutter and appropriate cutoff filters. The bandwidth used throughout the pulse radiolysis experiments was 5 nm. The radiation dose per pulse was monitored by means of a charge collector placed behind the irradiation cell and calibrated with a N_2O-saturated solution containing 0.1 M HCO_2^- and 0.5 mM methyl viologen with $G\varepsilon = 9.66\times10^{-4}$ m^2 J^{-1} at 602 nm.[36] G(X) represents the number of moles of species X formed or consumed per joule of energy absorbed by the system.

Continuous radiolysis: Continuous radiolysis was performed at room temperature (22±2°C) on 4 mL samples in a ^{60}Co-Gammacell with dose rates of 12–13 Gy min^{-1}. The absorbed radiation dose was determined with the Fricke chemical dosimeter by taking $G(Fe^{3+}) = 1.61$ μmol J^{-1}.[37] The reactions of **8** with e_{aq}^- were investigated in deaerated aqueous solutions containing 1.5 mM substrate and 0.25 M *t*BuOH in the presence or absence of $K_4[Fe(CN)_6]$ (4 mM) at pH≈7. The crude reaction mixture was passed through an ion-exchange resin (Amberlite IRA-400), to eliminate the iron salts, and monitored by HPLC on a C18-reverse-phase column as described above. Products were identified and quantified by comparison with authentic samples.

Steady-state photolysis: Aqueous solutions (10 mL) containing bromide **8** (≈1 mM) were irradiated under N_2 through quartz inside a Luzchem multilamp photoreactor, with light from twelve 8 W lamps emitting mainly at $\lambda = 254$ nm. The two cyclic diastereoisomers **21** and **23** were obtained as pure materials from the crude reaction mixture (by irradiation of **8** in the presence of iodide ion) employing preparative reverse-phase HPLC (Waters column, Spherisorb, 250×10 mm, 10 mm) and were spectroscopically characterized.

Synthesis of 8-Bromo-2′-deoxyinosine (8): Sodium nitrite (≈20 equiv) was added to a suspension of **1** (0.303 mmol) in glacial acetic acid (5 mL), and the mixture was stirred for 1.5 h. At the end of the reaction, the solution was neutralized with 1 M NaOH (≈82 mL) and evaporated to dryness in vacuo. The residue was purified by using reverse-phase chromatography (silica gel, aqueous acetonitrile (0 to 5%)). Two fractions were obtained: 8-bromohypoxanthine (**27**) and partially impure **8**. The latter was recrystallized from acetonitrile/water to obtain the pure compound. The overall yield for **8** was ≈30%. ^{1}H NMR (300 MHz, [D$_7$]DMSO): δ=8.08 (s, 1H; H2), 6.28 (t, J(H′,H2″)=7.1 Hz, 1H; H1′), 5.40 (d, J=4.5 Hz, 1H; OH3′), 4.90 (t, J=5.9 Hz, 1H; OH5′), 4.45 (m, 1H; H3′), 3.84 (td, J(H$_4$′,H5′)=5.2 Hz, J(H4′,H3′)=3.3 Hz, 1H; H4′), 3.62 (dt, J(H5′,H5″)=−12.0 Hz, J(H5′,H4′)=5.2 Hz, 1H; H5′), 3.5 (m, 1H; H5″), 3.17 (m, 1H; H2′), 2.23 ppm (ddd, J(H2″,H2′)=−13.3 Hz, J(H2″,H3′)=3.3 Hz, J(H2″,H1′)=7.1 Hz, 1H; H2″); ^{13}C NMR (75.5 MHz, [D$_7$]DMSO): δ=37.0 (C2′), 61.9 (C5′), 70.9 (C3′), 86.0 (C1′), 88.1 (C4′), 125.4 (C5), 125.6 (C8), 146.0 (C4), 149.1 (C2), 155.3 ppm (C=O); UV/Vis: λ_{max} (ε)=255 nm (1.35×10^4 M^{-1}cm^{-1}) at pH 7; MS (ESI): m/z: 331 (333) $[M+H]^+$; HRMS (FAB): calcd for $C_{10}H_{11}BrN_4O_4$: 331.0042; found: 331.0038 $[M+H]^+$.

(5′*R*)-5′,8-Cyclo-2′-deoxyinosine (21): ^{1}H NMR (300 MHz, [D$_7$]DMSO): δ=8.00 (s, 1H; H2), 6.42 (d, J(H1′,H2″)=4.8 Hz, 1H; H1′), 6.20 (d, J=6.0 Hz, 1H; OH5′), 5.43 (d, J=3.6 Hz, 1H; OH3′), 4.57 (dd, J=6.0, J(H5′,H4′)=0.6 Hz, 1H; H5′), 4.43 (d, J(H4′,H5′)=0.6 Hz, 1H; H4′), 4.20 (m, 1H; H3′), 2.31 (dd, J(H2′,H2″)=−13.4 Hz, J(H2′,H3′)=7.2 Hz, 1H; H2′), 2.00 ppm (dt, J(H2″,H2′)=−13.4 Hz, J(H2″,H1′) =J(H2″,H3′)=4.8 Hz, 1H; H2″); ^{13}C NMR (75.5 MHz, [D$_7$]DMSO): δ=44.8 (C2′), 64.9 (C5′), 69.7 (C3′), 84.7 (C1′), 90.1 (C4′), 123.8 (C5), 145.1 (C8), 145.6 (C4), 146.2 (C2), 156.9 ppm (C=O); MS (ESI): m/z: 251 $[M+H]^+$; HRMS (FAB): calcd for $C_{10}H_{10}N_4O_4$: 251.0780; found: 251.0764 $[M+H]^+$.

(5′*S*)-5′,8-Cyclo-2′-deoxyinosine (23): ^{1}H NMR (300 MHz, [D$_7$]DMSO): δ=7.99 (s, 1H; H2), 6.49 (d, J=6.3 Hz, 1H; OH5′), 6.37 (d, J(H1′,H2″)=4.8 Hz, 1H; H1′), 5.44 (d, J=4.5 Hz, 1H; OH3′), 5.01 (dd, J=6.3 Hz, J(H5′,H4′)=6.9 Hz, 1H; H5′), 4.63 (m, 1H; H3′), 4.49 (d, J(H4′,H5′)=6.9 Hz, 1H; H4′), 2.40 (dd, J(H2′,H2″)=−13.8 Hz, J(H2′,H3′)=7.5 Hz, 1H; H2′), 2.09 ppm (ddd, J(H2″,H2′)=−13.8 Hz, J(H2″,H1′)=4.8, J(H2″,H3′)=4.1 Hz, 1H; H2″); MS (ESI): m/z: 251 $[M+H]^+$; HRMS (FAB): calcd for $C_{10}H_{10}N_4O_4$: 251.0780; found: 251.0769 $[M+H]^+$.

Computational details: Hybrid meta-DFT calculations with the BB1K (Becke 88[38]-Becke 95[39] 1-parameter model for kinetics) functional[40] were carried out using the Gaussian 03 system of programs.[41] This HMDFT model was very recently tailored to give good reaction barrier heights.[40] An unrestricted wave function was used for radical species. Total energies were obtained employing the valence double-ζ basis set supplemented with polarization functions.[42,43] Addition of standard diffuse functions on heavy atoms[44,45] to better describe the anion states were found to give unreliable results as expected for radical anions that are unstable in the gas phase.[46] For example, the extra electron in the radical anion of **3** is localized at the diffuse s atomic orbitals of the carbon and nitrogen atoms of the C2-N10-H2 group. The use of moderate diffuse functions with a scaling factor λ of 0.7 provides reliable results according to the criterions previously outlined.[47] Hence the BB1K calculations were carried out with the 6-31+(λ=0.7)G** basis set. The geometry and the energy of the anions were calculated at fixed values of the C8−Br bond length. An increment step of 0.005 Å was used near the crossing points.

Acknowledgements

This work was supported in part by the European Community's Marie Curie Research Training Network under contract MRTN-CT-2003-505086 (CLUSTOXDNA). We also thank the financial support given by the Spanish MCYT (CTQ 2004-03811), the Generalitat Valenciana (Grupos 03/082, CTBPRB/2003/68, and Project GV04 A-349), the UPV (Project PPI-06-03), and Laboratori Fitocosmesi & Farmaceutici srl (Milan). We thank A. Monti and A. Martelli for assistance with pulse radiolysis experiments.

[1] R. Flyunt, R. Bazzanini, C. Chatgilialoglu, Q. G. Mulazzani, *J. Am. Chem. Soc.* **2000**, *122*, 4225–4226.
[2] C. Chatgilialoglu, M. Guerra, Q. G. Mulazzani, *J. Am. Chem. Soc.* **2003**, *125*, 3839–3848.
[3] C. Chatgilialoglu, M. Duca, C. Ferreri, M. Guerra, M. Ioele, Q. G. Mulazzani, H. Strittmatter, B. Giese, *Chem. Eur. J.* **2004**, *10*, 1249–1255.
[4] M. Ioele, R. Bazzanini, C. Chatgilialoglu, Q. G. Mulazzani, *J. Am. Chem. Soc.* **2000**, *122*, 1900–1907.
[5] C. Chatgilialoglu, C. Caminal, M. Guerra, Q. G. Mulazzani, *Angew. Chem.* **2005**, *117*, 6184–6186; *Angew. Chem. Int. Ed.* **2005**, *44*, 6030–6032.

[6] C. Chatgilialoglu, C. Caminal, A. Altieri, G. C. Vougioukalakis, Q. G. Mulazzani, T. Gimisis, M. Guerra, *J. Am. Chem. Soc.* **2006**, *128*, in press.
[7] L. B. Jimenez, S. Encinas, M. A. Miranda, M. L. Navacchia, C. Chatgilialoglu, *Photochem. Photobiol. Sci.* **2004**, *3*, 1042–1046.
[8] T. Kimura, K. Kawai, S. Tojo, T. Majima, *J. Org. Chem.* **2004**, *69*, 1169–1173.
[9] M. de Champdoré, L. De Napoli, D. Montesarchio, G. Piccialli, C. Caminal, Q. G. Mulazzani, M. L. Navacchia, C. Chatgilialoglu, *Chem. Commun.* **2004**, 1756–1757.
[10] A. Manetto, S. Breeger, C. Chatgilialoglu, T. Carell, *Angew. Chem.* **2006**, *118*, 325–328; *Angew. Chem. Int. Ed.* **2006**, *45*, 318–321.
[11] For selected recent papers on the transfer of excess electrons in DNA using 5-bromouracil moieties as the detection system, see: T. Ito, S. E. Rokita, *J. Am. Chem. Soc.* **2003**, *125*, 11480–11481; T. Ito, S. E. Rokita, *Angew. Chem.* **2004**, *116*, 1875–1878; *Angew. Chem. Int. Ed.* **2004**, *43*, 1839–1842; T. Ito, S. E. Rokita, *J. Am. Chem. Soc.* **2004**, *126*, 15552–15559; C. Wagner, H.-A. Wagenknecht, *Chem. Eur. J.* **2005**, *11*, 1871–1876; P. Kaden, E. Mayer-Enthart, A. Trifonov, T. Fiebing, H.-A. Wagenknecht, *Angew. Chem.* **2005**, *117*, 1620–1623; *Angew. Chem. Int. Ed.* **2005**, *44*, 1636–1639; E. Mayer-Enthart, P. Kaden, H.-A. Wagenknecht, *Biochemistry* **2005**, *44*, 11749–11757.
[12] R. E. Holmes, R. K. Robins, *J. Am. Chem. Soc.* **1964**, *86*, 1242–1245.
[13] F. Seela, C. Mittelbach, *Nucleosides Nucleotides* **1999**, *18*, 425–441.
[14] C. T. Aravindakumar, H. Mohan, M. Mudaliar, B. S. M. Rao, J. P. Mittal, M. N. Schuchmann, C. von Sonntag, *Int. J. Radiat. Biol.* **1994**, *66*, 351–365.
[15] a) L. P. Candeias, S. Steenken, *J. Am. Chem. Soc.* **1989**, *111*, 1094–1099; b) S. V. Jovanovic, M. G. Simic, *J. Phys. Chem.* **1986**, *90*, 974–978.
[16] a) G. V. Buxton, C. L. Greenstock, W. P. Helman, A. B. Ross, *J. Phys. Chem. Ref. Data* **1988**, *17*, 513–886; b) A. B. Ross, W. G. Mallard, W. P. Helman, G. V. Buxton, R. E. Huie, P. Neta, *NDRL-NIST Solution Kinetic Database—Version 3*, Notre Dame Radiation Laboratory, Notre Dame, IN and NIST Standard Reference Data, Gaithersburg, MD, **1998**.
[17] L. Wojnárovits, E. Takács, K. Dajka, S. S. Emmi, M. Russo, M. D'Angelantonio, *Radiat. Phys. Chem.* **2004**, *69*, 217–219.
[18] The rate constants for the reaction of the HO• radical with inosine is $4.4\times10^{9}\,\text{M}^{-1}\text{s}^{-1}$.[16] A similar value can be assumed for the analogous reaction of 8-bromo derivatives **8** or **12**. Therefore, more than 97% of HO• radicals are expected to be scavenged by *t*BuOH when [**8**] or $[\mathbf{12}]\leq1\times10^{-3}\,\text{M}$.
[19] G. L. Hug, *Natl. Stand. Ref. Data Ser. (US Natl. Bur. Stand.)* **1981**, *69*, 1–159.
[20] For example, see: G. V. Buxton, Q. G. Mulazzani, A. B. Ross, *J. Phys. Chem. Ref. Data* **1995**, *24*, 1055–1349.
[21] a) All redox potentials are versus NHE; b) P. Wardman, *J. Phys. Chem. Ref. Data* **1989**, *18*, 1637–1755.
[22] S. Fujita, S. Steenken, *J. Am. Chem. Soc.* **1981**, *103*, 2540–2545; S. Steenken, A. J. S. C. Vieira, *Angew. Chem.* **2001**, *113*, 581–583; *Angew. Chem. Int. Ed.* **2001**, *40*, 571–573.
[23] P. S. Rao, E. Hayon, *J. Phys. Chem.* **1975**, *79*, 1063–1066.
[24] Generally, electrophilic-type alkyl radicals, such as α-acyl derivatives, react with TMPD with a rate constant of $\approx10^{8}\,\text{M}^{-1}\text{s}^{-1}$. The rate constant of H• with TMPD is reported to be $2.2\times10^{8}\,\text{M}^{-1}\text{s}^{-1}$ at pH 1 where TMPD is doubly protonated.[16]
[25] Under the conditions employed: 1) the competition between **12** and TMPD for e_{aq}^{-} is well in favor of **12** because $k(e_{aq}^{-}+\text{TMPD})=9.1\times10^{7}\,\text{M}^{-1}\text{s}^{-1}$, (ref. [23]), and $[\mathbf{12}]\geq10\times[\text{TMPD}]$, and 2) although the rate constant of HO• with TMPD is $1.0\times10^{10}\,\text{M}^{-1}\text{s}^{-1}$,[16] the HO• radicals are still scavenged efficiently by *t*BuOH.[18]
[26] K. E. Hausler, W. J. Lorenz in *Standard Potentials in Aqueous Solution* (Eds.: A. J. Bard, R. Parsons, J. Jordan), Marcel Dekker, New York, **1985**, p. 408.
[27] T. Watanabe, K. Honda, *J. Phys. Chem.* **1982**, *86*, 2617–2619.
[28] For kinetic details of a similar mechanistic scheme, see: C. A. Kelly, E. L. Blinn, N. Camaioni, M. D'Angelantonio, Q. G. Mulazzani, *Inorg. Chem.* **1999**, *38*, 1579–1584; erratum: C. A. Kelly, E. L. Blinn, N. Camaioni, M. D'Angelantonio, Q. G. Mulazzani, *Inorg. Chem.* **1999**, *38*, 2756.
[29] G. E. Adams, R. L. Willson, *Trans. Faraday Soc.* **1969**, *65*, 2981–2987.
[30] S. Steenken, M. J. Davies, B. C. Gilbert, *J. Chem. Soc. Perkin Trans. 2* **1986**, 1003–1010.
[31] J. Grodkowski, P. Neta, C. J. Schlesener, J. K. Kochi, *J. Phys. Chem.* **1985**, *89*, 4373–4378.
[32] γ-Irradiation of aqueous solutions of $K_4[Fe(CN)_6]$ (4 mM) (reductant) continuously generates micromolar levels of the oxidant $[Fe(CN)_6]^{3-}$. Such a low concentration of oxidant should allow radical **10** to cyclize to radical **11** before being oxidized, thus improving the overall reaction performance.[2]
[33] A. Romieu, D. Gasparutto, J. Cadet, *Chem. Res. Toxicol.* **1999**, *12*, 412–421.
[34] a) L. P. Candeias, S. Steenken, *J. Phys. Chem.* **1992**, *96*, 937–944; b) L. P. Candeias, P. Wolf, P. O'Neill, S. Steenken, *J. Phys. Chem.* **1992**, *96*, 10302–10307.
[35] D. Enders, I. Breuer, E. Drosdow, *Synthesis* **2005**, 3239–3244.
[36] G. V. Buxton, Q. G. Mulazzani in *Electron Transfer in Chemistry. Vol. 1: Principles, Theories, Methods and Techniques* (Ed.: V. Balzani), Wiley-VCH, Weinheim, **2001**, pp. 503–557.
[37] J. W. T. Spinks, R. J. Woods, *An Introduction to Radiation Chemistry*, 3rd ed., Wiley, New York, **1990**, p. 100.
[38] A. D. Becke, *Phys. Rev. A* **1988**, *38*, 3098–3100.
[39] A. D. Becke, *J. Chem. Phys.* **1996**, *104*, 1040–1046.
[40] Y. Zhao, B. J. Lynch, D. G. Truhlar, *J. Phys. Chem. A* **2004**, *108*, 2715–2719.
[41] Gaussian 03, Revision B.5, M. J. Frisch, G. W. Trucks, H. B. Schlegel, G. E. Scuseria, M. A. Robb, J. R. Cheeseman, J. A. Montgomery, Jr., T. Vreven, K. N. Kudin, J. C. Burant, J. M. Millam, S. S. Iyengar, J. Tomasi, V. Barone, B. Mennucci, M. Cossi, G. Scalmani, N. Rega, G. A. Petersson, H. Nakatsuji, M. Hada, M. Ehara, K. Toyota, R. Fukuda, J. Hasegawa, M. Ishida, T. Nakajima, Y. Honda, O. Kitao, H. Nakai, M. Klene, X. Li, J. E. Knox, H. P. Hratchian, J. B. Cross, V. Bakken, C. Adamo, J. Jaramillo, R. Gomperts, R. E. Stratmann, O. Yazyev, A. J. Austin, R. Cammi, C. Pomelli, J. W. Ochterski, P. Y. Ayala, K. Morokuma, G. A. Voth, P. Salvador, J. J. Dannenberg, V. G. Zakrzewski, S. Dapprich, A. D. Daniels, M. C. Strain, O. Farkas, D. K. Malick, A. D. Rabuck, K. Raghavachari, J. B. Foresman, J. V. Ortiz, Q. Cui, A. G. Baboul, S. Clifford, J. Cioslowski, B. B. Stefanov, G. Liu, A. Liashenko, P. Piskorz, I. Komaromi, R. L. Martin, D. J. Fox, T. Keith, M. A. Al-Laham, C. Y. Peng, A. Nanayakkara, M. Challacombe, P. M. W. Gill, B. Johnson, W. Chen, M. W. Wong, C. Gonzalez, J. A. Pople, Gaussian, Inc., Wallingford CT, **2004**.
[42] P. C. Hariharan, J. A Pople, *Theor. Chim. Acta* **1973**, *28*, 213–222.
[43] M. M. Francl, W. J. Pietro, W. J. Hehre, J. S. Binkley, M. S. Gordon, D. J. DeFrees, J. A. Pople, *J. Chem. Phys.* **1982**, *77*, 3654–3665.
[44] T. Clark, J. Chandrasekhar, G. W. Spitznagel, P. von R. Schleyer, *J. Comput. Chem.* **1983**, *4*, 294–301.
[45] P. M. W. Gill, B. G. Johnson, J. A. Pople, M. J. Frisch, *Chem. Phys. Lett.* **1992**, *197*, 499–505.
[46] M. Guerra, *Chem. Phys. Lett.* **1990**, *167*, 315–319.
[47] M. Guerra, *J. Phys. Chem. A* **1999**, *103*, 5983–5988.

Received: January 10, 2006
Published online: July 5, 2006

Please note: Minor changes have been made to this manuscript since its publication in *Chemistry—A European Journal* Early View. The Editor.

